Measurement of Polarization Observables for the reaction $\gamma p \rightarrow K^0\Sigma^+$

Frank Gonzalez

Florida State University, Tallahassee, FL

11/14/2019

Outline

Outline

Why $\gamma p \rightarrow K^0\Sigma^+$?

- Photoproduction of neutral kaons offers advantage over charged ones since photons cannot couple directly to (vanishing) charge of the meson.
- Data on isospin related channels $K^0\Sigma^+$ and $K^+\Sigma^0$ allow for disentanglement of contributions from N^* and Δ^* resonances.

Why $\gamma p \to K^0\Sigma^+$?

- Photoproduction of neutral kaons offers advantage over charged ones since photons cannot couple directly to (vanishing) charge of the meson.
- Data on isospin related channels $K^0\Sigma^+$ and $K^+\Sigma^0$ allow for disentanglement of contributions from N^* and Δ^* resonances.
- Hyperon decay allows measurement of asymmetries, which allow for the extraction of hyperon recoil polarization P.
- Trade-off however is low cross-sections, leading to less statistics.
- The determination of the polarization observables allows for an understanding of the intermediate steps involved in the reaction.

Outline

$K^0\Sigma^+$ channel

- CLAS-g12 data were used for this analysis.

$K^0\Sigma^+$ channel

- CLAS-g12 data were used for this analysis.
- The outgoing Σ^+ is produced via strong force decay from N^*. Σ^+ then decays independently into a proton and a π^0 via the weak force.

$K^0\Sigma^+$ channel

- CLAS-g12 data were used for this analysis.
- The outgoing Σ^+ is produced via strong force decay from N^*. Σ^+ then decays independently into a proton and a π^0 via the weak force.
- Weak decay violates parity, thus allowing for extraction of polarization P observable of Σ^+ from angular distribution of a decay product in Σ^+ rest-frame.

$K^0\Sigma^+$ channel

- CLAS-g12 data were used for this analysis.
- The outgoing Σ^+ is produced via strong force decay from N^*. Σ^+ then decays independently into a proton and a π^0 via the weak force.
- Weak decay violates parity, thus allowing for extraction of polarization P observable of Σ^+ from angular distribution of a decay product in Σ^+ rest-frame.
- These observables are sensitive to interference from different states.

		Status as seen in										
Particle	J^P	overall	$N\gamma$	$N\pi$	$\Delta\pi$	$N\sigma$	$N\eta$	ΛK	ΣK	$N\rho$	$N\omega$	$N\eta'$
N	$1/2^+$	****										
$N(1440)$	$1/2^+$	****	****	****	****	**	****					
$N(1520)$	$3/2^-$	****	****	****	****	***						
$N(1535)$	$1/2^-$	****	****	****	***	*	****					
$N(1650)$	$1/2^-$	****	****	****	***	*	****	*				
$N(1675)$	$5/2^-$	****	****	****	****	***						
$N(1680)$	$5/2^+$	****	****	****	****	***						
$N(1700)$	$3/2^-$	***	**	***	***	*	*			*		
$N(1710)$	$1/2^+$	****	****	****	*		***	**	*	*	*	
$N(1720)$	$3/2^+$	****	****	****	***	*	*	****	*	*	*	
$N(1860)$	$5/2^+$	**	*	**		*	*					
$N(1875)$	$3/2^-$	***	**	**	*	**	*	*	*	*	*	
$N(1880)$	$1/2^+$	***	**	*	**	*	*	**	**		**	
$N(1895)$	$1/2^-$	****	****	*	*	*	****	**	**	*	*	****
$N(1900)$	$3/2^+$	****	****	**	**	*	*	**	**		*	**
$N(1990)$	$7/2^+$	**	**	**			*	*	*			
$N(2000)$	$5/2^+$	**	**	*	**	*	*				*	
$N(2040)$	$3/2^+$	*		*								
$N(2060)$	$5/2^-$	***	***	**	*	*	*	*	*	*	*	
$N(2100)$	$1/2^+$	***	**	***	**	**	*	*		*	*	**
$N(2120)$	$3/2^-$	***	***	**	**	**		**	*		*	*
$N(2190)$	$7/2^-$	****	****	****	****	**	*	**	*	*	*	
$N(2220)$	$9/2^+$	****	**	****			*	*	*			
$N(2250)$	$9/2^-$	****	**	****			*	*	*			
$N(2300)$	$1/2^+$	**		**								
$N(2570)$	$5/2^-$	**		**								
$N(2600)$	$11/2^-$	***		***								
$N(2700)$	$13/2^+$	**		**								
****	Existence is certain.											
***	Existence is very likely.											
**	Evidence of existence is fair.											
*	Evidence of existence is poor.											

Figure 1: Particle Data Group.

Outline

Polarization Observables

- Real photoproduction of pseudoscalar mesons may be described in full by 16 observables. At least 8 observables are needed due to parity conservation.

Polarization Observables

- Real photoproduction of pseudoscalar mesons may be described in full by 16 observables. At least 8 observables are needed due to parity conservation.
- Double polarization observables C_x and C_z characterize reactions under distinct combinations of two of the following: **beam**, target and **baryon recoil polarization**.

Polarization Observables

- Real photoproduction of pseudoscalar mesons may be described in full by 16 observables. At least 8 observables are needed due to parity conservation.
- Double polarization observables C_x and C_z characterize reactions under distinct combinations of two of the following: **beam**, target and **baryon recoil polarization**.
- Photon polarization in g12 data allows for study of strangeness in Σ^+ hyperon, along with extraction of C_x and C_z.

Polarization Observables

- Real photoproduction of pseudoscalar mesons may be described in full by 16 observables. At least 8 observables are needed due to parity conservation.
- Double polarization observables C_x and C_z characterize reactions under distinct combinations of two of the following: **beam**, target and **baryon recoil polarization**.
- Photon polarization in g12 data allows for study of strangeness in Σ^+ hyperon, along with extraction of C_x and C_z.
- Circularly polarized photons may have their polarization transferred fully or partially to spin orientation of hyperons within reaction plane.

Polarization Observables

- Real photoproduction of pseudoscalar mesons may be described in full by 16 observables. At least 8 observables are needed due to parity conservation.
- Double polarization observables C_x and C_z characterize reactions under distinct combinations of two of the following: **beam**, target and **baryon recoil polarization**.
- Photon polarization in g12 data allows for study of strangeness in Σ^+ hyperon, along with extraction of C_x and C_z.
- Circularly polarized photons may have their polarization transferred fully or partially to spin orientation of hyperons within reaction plane.
- The C_x and C_z double polarization observables allow for a characterization of the transferred polarization from incident beam to recoiling hyperon along the orthonormal axes in the scattering plane.

Polarization Observables

Spin-Dependent Cross-Section for $K^0\Sigma^+$ Photoproduction

$$\rho_Y \frac{d\sigma}{d\Omega_{K^+}} = \left.\frac{d\sigma}{d\Omega_{K^+}}\right|_{\text{unpol}} \{1 + \sigma_y P + P_\odot(C_x\sigma_x + C_z\sigma_z)\}$$

$$\rho_Y = (1 + \vec{\sigma} \cdot \vec{P}_Y)$$

Polarization Observables

Spin-Dependent Cross-Section for $K^0\Sigma^+$ Photoproduction

$$\rho_Y \frac{d\sigma}{d\Omega_{K^+}} = \left.\frac{d\sigma}{d\Omega_{K^+}}\right|_{\text{unpol}} \{1 + \sigma_y P + P_\odot(C_x\sigma_x + C_z\sigma_z)\}$$

$$\rho_Y = (1 + \vec{\sigma} \cdot \vec{P}_Y)$$

Polarization Components

$$P_{\Sigma_x^+} = P_\odot C_x$$

$$P_{\Sigma_y^+} = P$$

$$P_{\Sigma_z^+} = P_\odot C_z$$

Polarization Observables

Spin-Dependent Cross-Section for $K^0\Sigma^+$ Photoproduction

$$\rho_Y \frac{d\sigma}{d\Omega_{K^+}} = \left.\frac{d\sigma}{d\Omega_{K^+}}\right|_{\text{unpol}} \{1 + \sigma_y P + P_\odot(C_x\sigma_x + C_z\sigma_z)\}$$

$$\rho_Y = (1 + \vec{\sigma} \cdot \vec{P}_Y)$$

Polarization Components

$$P_{\Sigma^+_x} = P_\odot C_x$$
$$P_{\Sigma^+_y} = P$$
$$P_{\Sigma^+_z} = P_\odot C_z$$

- Transverse (induced) polarization $P_{\Sigma^+_y}$ is equivalent to P observable.
- The $\hat{x}$ and $\hat{z}$ components of hyperon polarization are proportional to C_x, C_z via degree of beam polarization $P_\odot$.

Polarization Observables: Reference Frames

- Measurement of observables is based on the axes of the scattering plane.

Polarization Observables: Reference Frames

- Measurement of observables is based on the axes of the scattering plane.
- Production plane is defined by momentum vectors of incoming photon and outgoing Σ^+ in the CM-frame of $\gamma p \rightarrow K^0\Sigma^+$.

Polarization Observables: Reference Frames

- Measurement of observables is based on the axes of the scattering plane.
- Production plane is defined by momentum vectors of incoming photon and outgoing Σ^+ in the CM-frame of $\gamma p \to K^0\Sigma^+$.
- Hyperon polarization within production plane can be described with respect to given z axis along direction of beam in overall CM-frame.

Polarization Observables: Reference Frames

- Measurement of observables is based on the axes of the scattering plane.
- Production plane is defined by momentum vectors of incoming photon and outgoing Σ^+ in the CM-frame of $\gamma p \to K^0\Sigma^+$.
- Hyperon polarization within production plane can be described with respect to given z axis along direction of beam in overall CM-frame.

Scattering Frame

$$\gamma(k) + p(q_1) \to K^0(q_2) + \Sigma^+(q_3),$$

$$\hat{y} = \frac{\vec{k} \times \vec{q_2}}{|\vec{k} \times \vec{q_2}|}, \qquad \hat{z} = \frac{\vec{k}}{|\vec{k}|}, \qquad \hat{x} = \vec{y} \times \vec{z}.$$

Polarization Observables: Reference Frames

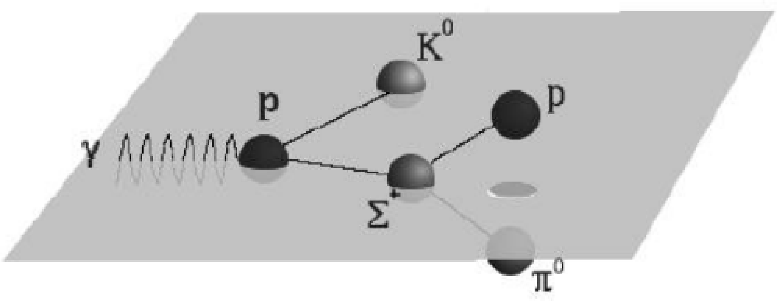

Figure 2: Scattering plane of $\gamma p \to K^0\Sigma^+$.

Outline

The g12 Experiment using CLAS@JLab

- g12 experiment was conducted in Hall B using the CEBAF Large Acceptance Spectrometer (CLAS).

The g12 Experiment using CLAS@JLab

- g12 experiment was conducted in Hall B using the CEBAF Large Acceptance Spectrometer (CLAS).

g12 experiment specs

Photon polarization: Circular.
Target Material: Liquid hydrogen.
Target position: 90 cm from CLAS detector center.
Energy range: 1.1 – 5.4 GeV.

The g12 Experiment using CLAS@JLab

- g12 experiment was conducted in Hall B using the CEBAF Large Acceptance Spectrometer (CLAS).

g12 experiment specs

Photon polarization: Circular.
Target Material: Liquid hydrogen.
Target position: 90 cm from CLAS detector center.
Energy range: 1.1 – 5.4 GeV.

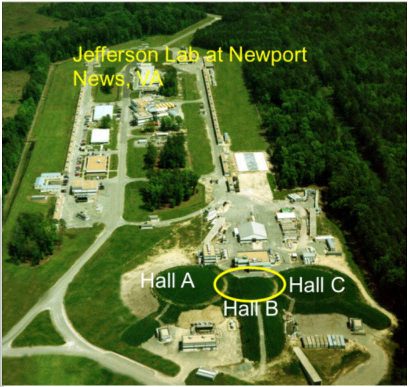

Figure 3: Hall B at JLab, home to the g12 experiment.

Outline

$\gamma p \rightarrow K^0\Sigma^+$, Event Selection and Cuts

- All analysis and data cuts have been applied by the collaboration; 3 π's data set approved in analysis.

$\gamma p \rightarrow K^0\Sigma^+$, Event Selection and Cuts

- All analysis and data cuts have been applied by the collaboration; 3 π's data set approved in analysis.
- Trigger required either:

$\gamma p \rightarrow K^0\Sigma^+$, Event Selection and Cuts

- All analysis and data cuts have been applied by the collaboration; 3 π's data set approved in analysis.
- Trigger required either:
  - Three charged tracks with no restriction on beam energy.

$\gamma p \rightarrow K^0\Sigma^+$, Event Selection and Cuts

- All analysis and data cuts have been applied by the collaboration; 3 π's data set approved in analysis.
- Trigger required either:
  - Three charged tracks with no restriction on beam energy.
  - Two tracks with restriction of having at least a photon with energy $E_\gamma > 3.6$ GeV.

$\gamma p \rightarrow K^0\Sigma^+$, Event Selection and Cuts

- All analysis and data cuts have been applied by the collaboration; 3 π's data set approved in analysis.
- Trigger required either:
  - Three charged tracks with no restriction on beam energy.
  - Two tracks with restriction of having at least a photon with energy $E_\gamma > 3.6$ GeV.
- Raw data underwent reconstruction to yield sensible physical quantities: particle IDs, angles, momenta and energies.

$\gamma p \to K^0\Sigma^+$, Event Selection and Cuts

- All analysis and data cuts have been applied by the collaboration; 3 π's data set approved in analysis.
- Trigger required either:
  - Three charged tracks with no restriction on beam energy.
  - Two tracks with restriction of having at least a photon with energy $E_\gamma > 3.6$ GeV.
- Raw data underwent reconstruction to yield sensible physical quantities: particle IDs, angles, momenta and energies.

g12 Data Cuts

- **Vertex Cut:** -110.0 cm $<$ z-vertex $<$ -70.0 cm.
- **Timing Cut:** $|\Delta_{\mathrm{TBID}}| < 1$ ns.
- **Particle ID Cut:** $\Delta\beta = |\beta_{\mathrm{c}} - \beta_{\mathrm{m}}| \leq 3\sigma$.
- **Fiducial Cut:** nominal scenario.

$\gamma p \to K^0\Sigma^+$, Data Cuts

- **Energy-Loss Correction:** 4-vectors of final-state particles were modified event-by-event in order to account for lost energy and momentum of each particles in the materials it had interacted with.

$\gamma p \rightarrow K^0\Sigma^+$, Data Cuts

- **Energy-Loss Correction:** 4-vectors of final-state particles were modified event-by-event in order to account for lost energy and momentum of each particles in the materials it had interacted with.
- **Kinematic Fitting:** modified raw 4-vectors by imposing energy-momentum conservation as a physical constraint. CLAS detector cannot detect π^0, it can only detect the π^0 in the very forward direction. Missing mass/momentum thus determined from measured three-momenta and energies of measured particles.

$\gamma p \to K^0\Sigma^+$, Data Cuts

- **Energy-Loss Correction:** 4-vectors of final-state particles were modified event-by-event in order to account for lost energy and momentum of each particles in the materials it had interacted with.
- **Kinematic Fitting:** modified raw 4-vectors by imposing energy-momentum conservation as a physical constraint. CLAS detector cannot detect π^0, it can only detect the π^0 in the very forward direction. Missing mass/momentum thus determined from measured three-momenta and energies of measured particles.

Missing Momentum

$$x^\mu = k^\mu + P^\mu - \sum_{i=1}^{2,3} p_i^\mu .$$

Missing Mass

$$m_X^2 = x^\mu x_\mu .$$

$\gamma p \rightarrow K^0\Sigma^+$: Q-factor

- Considered two different mass cuts before applying the background subtraction:

$\gamma p \to K^0\Sigma^+$: Q-factor

- Considered two different mass cuts before applying the background subtraction:
  - Strangeness conserved in EM and strong interactions. Applied a narrow cut of 30 MeV around K^0 mass of 500 MeV to enhance Σ^+ peak of q-values.

$\gamma p \to K^0\Sigma^+$: Q-factor

- Considered two different mass cuts before applying the background subtraction:
    - Strangeness conserved in EM and strong interactions. Applied a narrow cut of 30 MeV around K^0 mass of 500 MeV to enhance Σ^+ peak of q-values.
    - Dominant reaction contributing to $p\pi^+\pi^-\pi^0$ is ω. Applied mass cut to remove contributions from ω: $m_{\pi^+\pi^-\pi^0} < 752$ MeV and $m_{\pi^+\pi^-\pi^0} < 812$ MeV.

$\gamma p \to K^0\Sigma^+$: Q-factor

- Considered two different mass cuts before applying the background subtraction:
    - Strangeness conserved in EM and strong interactions. Applied a narrow cut of 30 MeV around K^0 mass of 500 MeV to enhance Σ^+ peak of q-values.
    - Dominant reaction contributing to $p\pi^+\pi^-\pi^0$ is ω. Applied mass cut to remove contributions from ω: $m_{\pi^+\pi^-\pi^0} < 752$ MeV and $m_{\pi^+\pi^-\pi^0} < 812$ MeV.
- **Q-factor method:** Removal of background underneath signal peak. Event-based method.

$\gamma p \to K^0\Sigma^+$: Q-factor

- Considered two different mass cuts before applying the background subtraction:
  - Strangeness conserved in EM and strong interactions. Applied a narrow cut of 30 MeV around K^0 mass of 500 MeV to enhance Σ^+ peak of q-values.
  - Dominant reaction contributing to $p\pi^+\pi^-\pi^0$ is ω. Applied mass cut to remove contributions from ω: $m_{\pi^+\pi^-\pi^0} < 752$ MeV and $m_{\pi^+\pi^-\pi^0} < 812$ MeV.
- **Q-factor method:** Removal of background underneath signal peak. Event-based method.
- Q-factor used as event weight in order to determine signal contribution to physical distributions.

$\gamma p \to K^0\Sigma^+$: Q-factor

- Considered two different mass cuts before applying the background subtraction:
  - Strangeness conserved in EM and strong interactions. Applied a narrow cut of 30 MeV around K^0 mass of 500 MeV to enhance Σ^+ peak of q-values.
  - Dominant reaction contributing to $p\pi^+\pi^-\pi^0$ is ω. Applied mass cut to remove contributions from ω: $m_{\pi^+\pi^-\pi^0} < 752$ MeV and $m_{\pi^+\pi^-\pi^0} < 812$ MeV.
- **Q-factor method:** Removal of background underneath signal peak. Event-based method.
- Q-factor used as event weight in order to determine signal contribution to physical distributions.
- Due to $K^0 \to \pi^+\pi^-$ and $\Sigma^+ \to p\pi^0$ correlation, reference quantity can be either invariant mass.

Q-factor background subtraction

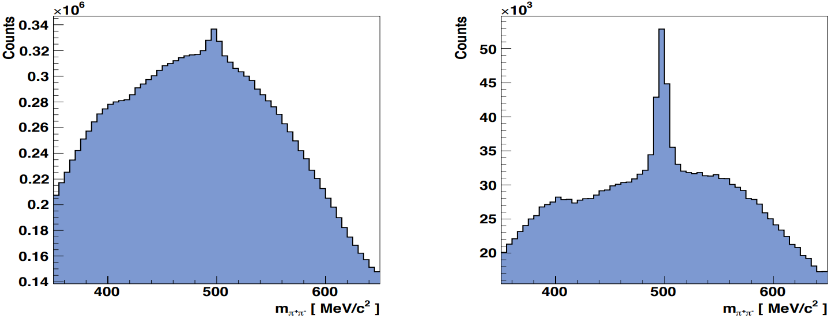

Figure 4: **Left:** Raw distribution of all g12 $\pi^+\pi^-\pi^0$ events. **Right:** Same invariant mass $\pi^+\pi^-$ after Σ^+ mass-cut has been employed.

Q-factor background subtraction

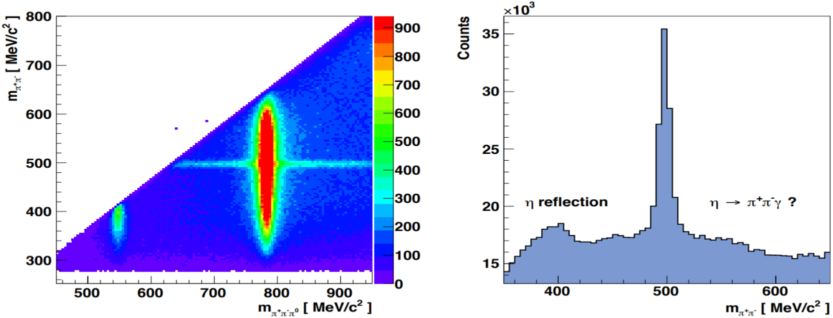

Figure 5: **Left:** Invariant $\pi^+\pi^-\pi^0$ mass vs. $\pi^+\pi^-$ mass for all g12 $\pi^+\pi^-\pi^0$ events. **Right:** Same invariant $\pi^+\pi^-$ mass distribution after the ω and Σ^+ mass-cuts.

$\gamma p \rightarrow K^0\Sigma^+$: Q-factor background subtraction

- In order to subtract background for $K^0\Sigma^+$ final state, g12 data was divided into 50 MeV-wide and 100 MeV-wide incident photon energy for cross-section and induced polarization measurements, respectively.

$\gamma p \to K^0\Sigma^+$: Q-factor background subtraction

- In order to subtract background for $K^0\Sigma^+$ final state, g12 data was divided into 50 MeV-wide and 100 MeV-wide incident photon energy for cross-section and induced polarization measurements, respectively.
- Complete set of invariant $\pi^+\pi^-$ and $p\pi^0$ mass-distributions for 50-MeV-wide incident-photon energy bins in range $E_\gamma \in [1100, 3000]$ MeV.

$\gamma p \rightarrow K^0\Sigma^+$: Q-factor background subtraction

- In order to subtract background for $K^0\Sigma^+$ final state, g12 data was divided into 50 MeV-wide and 100 MeV-wide incident photon energy for cross-section and induced polarization measurements, respectively.
- Complete set of invariant $\pi^+\pi^-$ and $p\pi^0$ mass-distributions for 50-MeV-wide incident-photon energy bins in range $E_\gamma \in [1100, 3000]$ MeV.
- The invariant $p\pi^0$ mass was used as the reference coordinate for the determination of the Q-value for the polarization observables.

$\gamma p \to K^0\Sigma^+$: Q-factor background subtraction

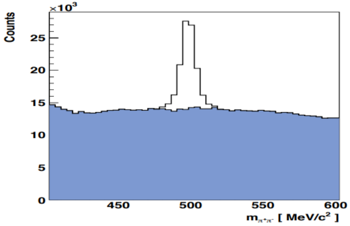

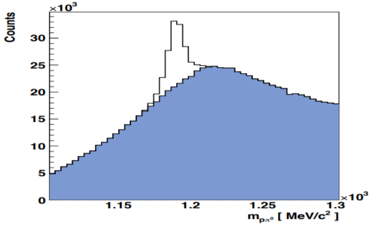

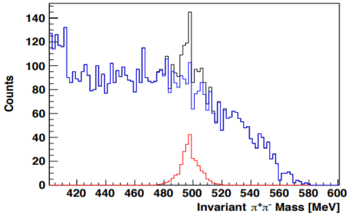

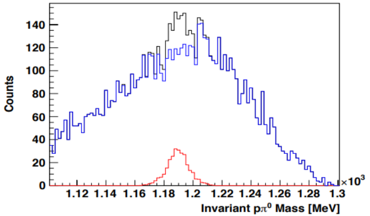

$\gamma p \to K^0\Sigma^+$: Q-factor background subtraction

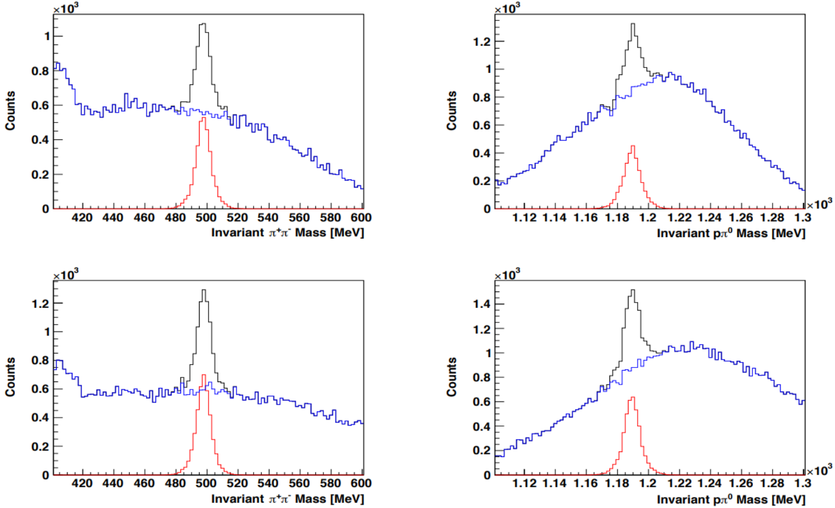

$\gamma p \rightarrow K^0\Sigma^+$: Q-factor background subtraction

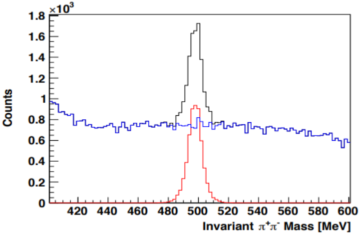

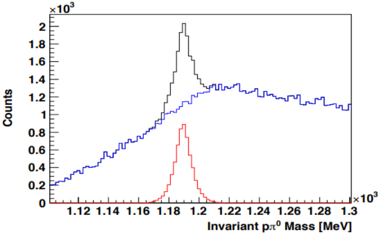

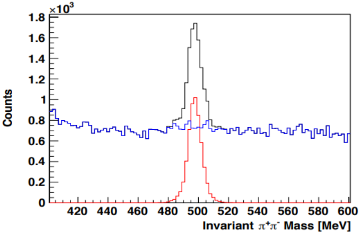

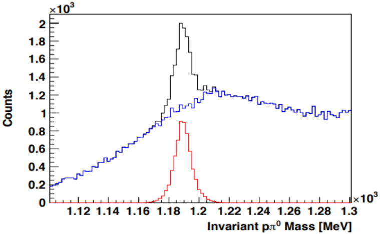

$\gamma p \rightarrow K^0 \Sigma^+$: Q-factor background subtraction

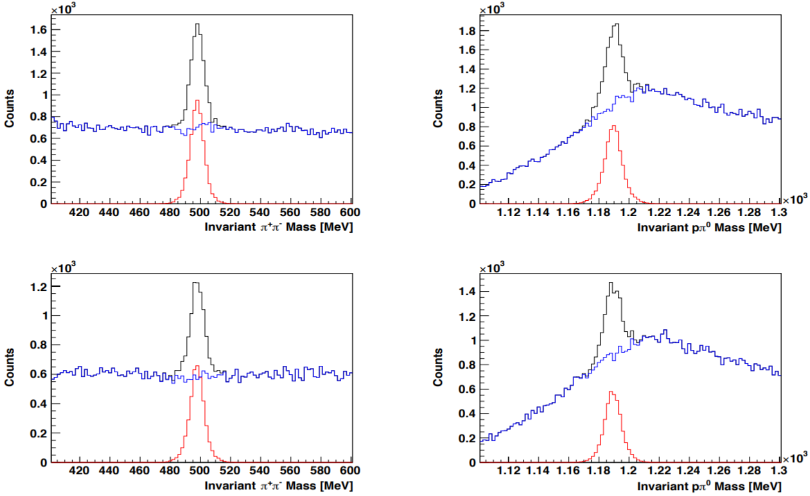

Outline

1. Introduction
   - The Reaction, $\gamma p \to K^0\Sigma^+$
   - The Spectroscopy of Baryon Resonances
   - The Formalism of Hyperon Polarization
2. Experimental Approach and Data Analysis
   - The Experiment
   - The Reaction
   - The Extraction of Polarization Observables
3. Summary and Outlook
   - Summary

Extracting the P Observable

- Once clean $K^0\Sigma^+$ events have been selected, one can proceed to extract polarization observables for the Σ^+ hyperon. Part of Dr. Zulkaida's dissertation.

Extracting the P Observable

- Once clean $K^0\Sigma^+$ events have been selected, one can proceed to extract polarization observables for the Σ^+ hyperon. Part of Dr. Zulkaida's dissertation.
- Boosted all 4-momenta of particles of interest from Lab-frame to CM-frame, and then to Σ^+ rest frame.

Extracting the P Observable

- Once clean $K^0\Sigma^+$ events have been selected, one can proceed to extract polarization observables for the Σ^+ hyperon. Part of Dr. Zulkaida's dissertation.
- Boosted all 4-momenta of particles of interest from Lab-frame to CM-frame, and then to Σ^+ rest frame.
- Incident photon and recoiling Σ^+ define the reaction plane in the CM-frame.

Extracting the P Observable

- Once clean $K^0\Sigma^+$ events have been selected, one can proceed to extract polarization observables for the Σ^+ hyperon. Part of Dr. Zulkaida's dissertation.
- Boosted all 4-momenta of particles of interest from Lab-frame to CM-frame, and then to Σ^+ rest frame.
- Incident photon and recoiling Σ^+ define the reaction plane in the CM-frame.
- The measurement of the Σ^+ induced recoil polarization P was thus based on the asymmetry between the proton count rate above and below the reaction plane in the Σ^+ rest-frame.

Extracting the P Observable

- Once clean $K^0\Sigma^+$ events have been selected, one can proceed to extract polarization observables for the Σ^+ hyperon. Part of Dr. Zulkaida's dissertation.
- Boosted all 4-momenta of particles of interest from Lab-frame to CM-frame, and then to Σ^+ rest frame.
- Incident photon and recoiling Σ^+ define the reaction plane in the CM-frame.
- The measurement of the Σ^+ induced recoil polarization P was thus based on the asymmetry between the proton count rate above and below the reaction plane in the Σ^+ rest-frame.
- P observable does not require beam's polarization data; P can be seen as the "C_y" observable.

Extracting the P Observable

- Proton decay angles are measured in so-called Adair frame (z-axis is in direction of photon in overall CM-frame, while y-axis is orthogonal to reaction plane).

Extracting the P Observable

- Proton decay angles are measured in so-called Adair frame (z-axis is in direction of photon in overall CM-frame, while y-axis is orthogonal to reaction plane).
- Induced polarization P of Σ^+ determined by $\hat{y}$-component of the Σ^+ polarization. This is effectively defined by angle of outgoing proton w.r.t. scattering plane. Whether this angle was greater than or less than zero allowed us to determine if proton was above or below scattering plane,

Extracting the P Observable

- Proton decay angles are measured in so-called Adair frame (z-axis is in direction of photon in overall CM-frame, while y-axis is orthogonal to reaction plane).
- Induced polarization P of Σ^+ determined by $\hat{y}$-component of the Σ^+ polarization. This is effectively defined by angle of outgoing proton w.r.t. scattering plane. Whether this angle was greater than or less than zero allowed us to determine if proton was above or below scattering plane,

$$\cos\theta_y^p = \vec{p}_{\Sigma^+} \cdot \hat{y}$$

Extracting the P Observable

- Proton decay angles are measured in so-called Adair frame (z-axis is in direction of photon in overall CM-frame, while y-axis is orthogonal to reaction plane).
- Induced polarization P of Σ^+ determined by $\hat{y}$-component of the Σ^+ polarization. This is effectively defined by angle of outgoing proton w.r.t. scattering plane. Whether this angle was greater than or less than zero allowed us to determine if proton was above or below scattering plane,

$$\cos\theta_y^p = \vec{p}_{\Sigma^+} \cdot \hat{y}$$

- For the induced polarization, we integrate over all events above and below the reaction plane so that no direct angular dependence on the proton is needed for either observable C_x and C_z.

Extracting the P Observable, Histograms

- The task of measuring P thus reduces to a *counting experiment* with a degree of parity mixing of $\alpha = -0.98 \pm 0.016$,

Extracting the P Observable, Histograms

- The task of measuring P thus reduces to a *counting experiment* with a degree of parity mixing of $\alpha = -0.98 \pm 0.016$,

$$P = \frac{2}{\alpha} \cdot \frac{N_{\text{up}} - N_{\text{down}}}{N_{\text{up}} + N_{\text{down}}}$$

Extracting the P Observable, Histograms

- The task of measuring P thus reduces to a *counting experiment* with a degree of parity mixing of $\alpha = -0.98 \pm 0.016$,

$$P = \frac{2}{\alpha} \cdot \frac{N_{\text{up}} - N_{\text{down}}}{N_{\text{up}} + N_{\text{down}}}$$

- Hyperon polarization from CLAS g12, in 100-MeV-wide energy bins and covering an energy range of $1.15 < E_\gamma < 3.05$ GeV. Given uncertainties for g12 data are statistical uncertainties, whereas the Q-factor uncertainties are added in quadrature.

Extracting the P Observable, Histograms

- The task of measuring P thus reduces to a *counting experiment* with a degree of parity mixing of $\alpha = -0.98 \pm 0.016$,

$$P = \frac{2}{\alpha} \cdot \frac{N_{\text{up}} - N_{\text{down}}}{N_{\text{up}} + N_{\text{down}}}$$

- Hyperon polarization from CLAS g12, in 100-MeV-wide energy bins and covering an energy range of $1.15 < E_\gamma < 3.05$ GeV. Given uncertainties for g12 data are statistical uncertainties, whereas the Q-factor uncertainties are added in quadrature.
- Results already approved and included within analysis notes.

Extraction Methods for the C_x & C_z Observables

- Double polarization observables C_x and C_z have not been extracted for $\gamma p \to K^0\Sigma^+$ reaction.

Extraction Methods for the C_x & C_z Observables

- Double polarization observables C_x and C_z have not been extracted for $\gamma p \rightarrow K^0\Sigma^+$ reaction.
- Furthermore, beam polarization g12 data has not been used for the extraction of these observables; new addition to the analysis of $K^0\Sigma^+$.

Extraction Methods for the C_x & C_z Observables

- Double polarization observables C_x and C_z have not been extracted for $\gamma p \to K^0\Sigma^+$ reaction.
- Furthermore, beam polarization g12 data has not been used for the extraction of these observables; new addition to the analysis of $K^0\Sigma^+$.
- Asymmetry is calculated for proton angle bin $(\cos\theta_p)$ recording number of events as $N_\pm$ for positive/negative helicity states.

Extraction Methods for the C_x & C_z Observables

- Double polarization observables C_x and C_z have not been extracted for $\gamma p \to K^0\Sigma^+$ reaction.
- Furthermore, beam polarization g12 data has not been used for the extraction of these observables; new addition to the analysis of $K^0\Sigma^+$.
- Asymmetry is calculated for proton angle bin ($\cos\theta_p$) recording number of events as $N_\pm$ for positive/negative helicity states.
- Implemented two strategies in order to extract double polarization observables:

Extraction Methods for the C_x & C_z Observables

- Double polarization observables C_x and C_z have not been extracted for $\gamma p \rightarrow K^0\Sigma^+$ reaction.
- Furthermore, beam polarization g12 data has not been used for the extraction of these observables; new addition to the analysis of $K^0\Sigma^+$.
- Asymmetry is calculated for proton angle bin $(\cos\theta_p)$ recording number of events as $N_\pm$ for positive/negative helicity states.
- Implemented two strategies in order to extract double polarization observables:
    - **One-dimensional fit:** Individually yields C_x or C_z.

Extraction Methods for the C_x & C_z Observables

- Double polarization observables C_x and C_z have not been extracted for $\gamma p \rightarrow K^0\Sigma^+$ reaction.
- Furthermore, beam polarization g12 data has not been used for the extraction of these observables; new addition to the analysis of $K^0\Sigma^+$.
- Asymmetry is calculated for proton angle bin ($\cos\theta_p$) recording number of events as $N_\pm$ for positive/negative helicity states.
- Implemented two strategies in order to extract double polarization observables:
  - **One-dimensional fit:** Individually yields C_x or C_z.
  - **Maximum-likelihood fit:** Simultaneous extraction of all observables P, C_x and C_z.

One-Dimensional Fit

- For g12 experiment, electron-beam helicity flipped at 30 Hz rate.

One-Dimensional Fit

- For g12 experiment, electron-beam helicity flipped at 30 Hz rate.
- If beam helicity $P_{\odot}$ can be flipped, one can thus obtain C_i asymmetry as a function of proton angle $\cos\theta_p$. Asymmetry is related to angular distribution of proton as

$$A(\cos\theta^p_{x/z}) = \frac{N_+ - N_-}{N_+ + N_-} = \alpha P_{\odot} C_{x/z} \cos\theta^p_{x/z}.$$

Maximum-Likelihood Method

- Binning of data could hide some asymmetry features.

Maximum-Likelihood Method

- Binning of data could hide some asymmetry features.
- Maximum-likelihood method is an event-by-event method, requiring no binning and therefore preventing the possible loss of information and allowing simultaneous extraction of polarization observables.

Maximum-Likelihood Method

- Binning of data could hide some asymmetry features.
- Maximum-likelihood method is an event-by-event method, requiring no binning and therefore preventing the possible loss of information and allowing simultaneous extraction of polarization observables.
- Likelihood $\mathbb{L}$ (joint-probability density) for obtaining set of observed values in experiment, given specific set of polarization observables, is given by the product of probability density $\mathcal{P}_i$ for observing individual events.

Likelihood Function

$$\mathbb{L} = \prod_{i=1}^{N} \mathcal{P}_i$$

Maximum-Likelihood Method

- Binning of data could hide some asymmetry features.
- Maximum-likelihood method is an event-by-event method, requiring no binning and therefore preventing the possible loss of information and allowing simultaneous extraction of polarization observables.
- Likelihood $\mathbb{L}$ (joint-probability density) for obtaining set of observed values in experiment, given specific set of polarization observables, is given by the product of probability density $\mathcal{P}_i$ for observing individual events.

Likelihood Function

$$\mathbb{L} = \prod_{i=1}^{N} \mathcal{P}_i$$

Single Event Probability Distribution Function

$$\mathcal{P}(\cos\theta_x^p, \cos\theta_z^p, \cos\theta_y^p | C_x, C_z, P) = 1 \pm P_{\odot}\alpha(C_x \cos\theta_x^p + C_z \cos\theta_z^p) + \alpha P \cos\theta_y^p$$

Maximum-Likelihood Method

- Each given event has its own weight w_i, calculated via Q-factor method.

Maximum-Likelihood Method

- Each given event has its own weight w_i, calculated via Q-factor method.
- Computationally, it is convenient to minimize negative log-likelihood function as opposed to maximazing it.

Maximum-Likelihood Method

- Each given event has its own weight w_i, calculated via Q-factor method.
- Computationally, it is convenient to minimize negative log-likelihood function as opposed to maximazing it.

Probability Distribution Function

$$-\log \mathbb{L} = -\sum_{i=1}^{N} w_i \log(\mathcal{P}_i)$$

$$-\log \mathbb{L} = -\sum_{i=1}^{N} w_i \log(1 \pm P_{\odot}\alpha(C_x \cos\theta_x^p + C_z \cos\theta_z^p) + \alpha P \cos\theta_y^p)$$

Maximum-Likelihood Method (P Observable)

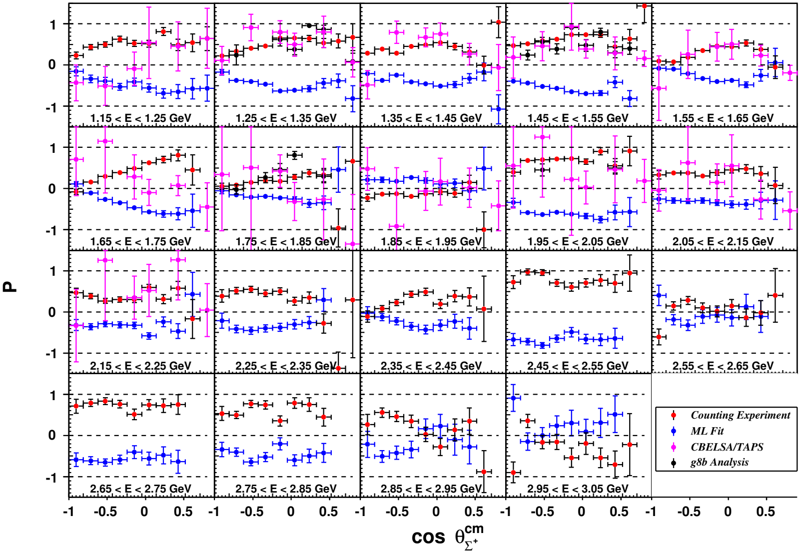

Maximum-Likelihood Method (C_x Observable)

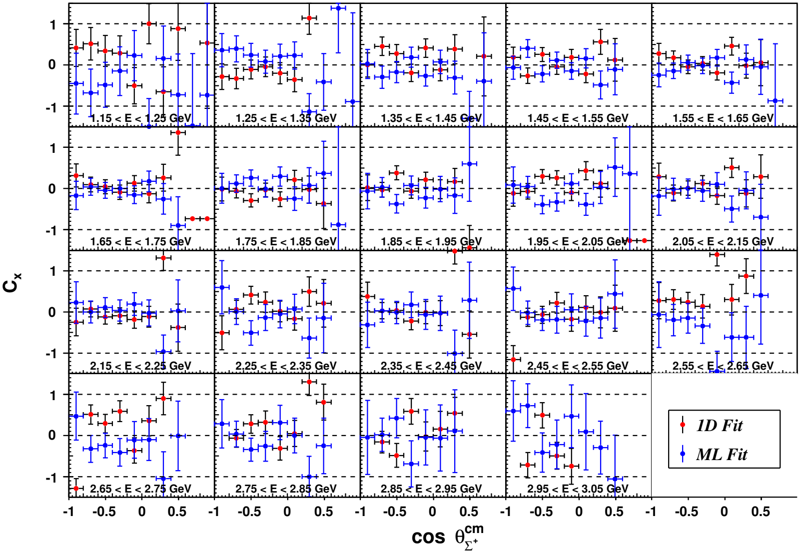

Maximum-Likelihood Method (C_z Observable)

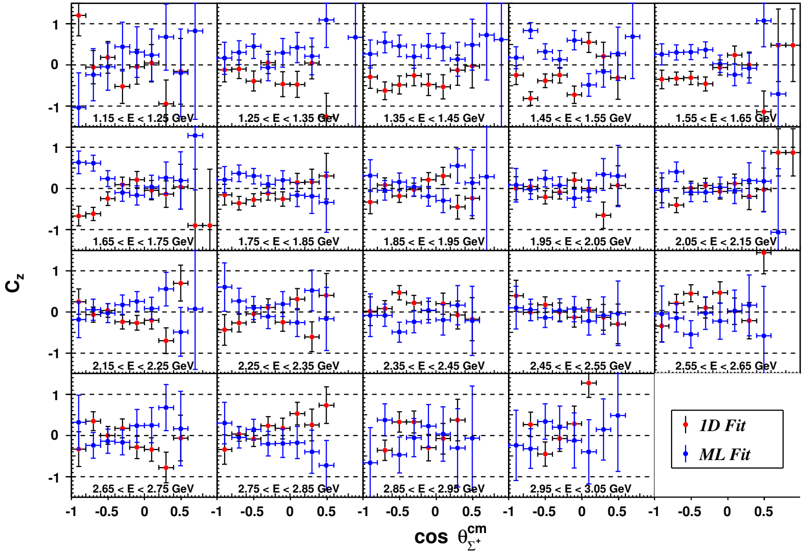

Outline

Summary

- The photoproduction of $K^0\Sigma^+$ is an unexplored and important channel to study due to its parity violation, allowing for the construction of an asymmetry, thus allowing for measurement of polarization observables.

Summary

- The photoproduction of $K^0\Sigma^+$ is an unexplored and important channel to study due to its parity violation, allowing for the construction of an asymmetry, thus allowing for measurement of polarization observables.
- Polarization observables allow for the disentanglement of N^* and Δ^* resonances.

Summary

- The photoproduction of $K^0\Sigma^+$ is an unexplored and important channel to study due to its parity violation, allowing for the construction of an asymmetry, thus allowing for measurement of polarization observables.
- Polarization observables allow for the disentanglement of N^* and Δ^* resonances.
- Determination of observables leads an understanding of the intermediate steps involved in the reaction of interest.

Summary

- The photoproduction of $K^0\Sigma^+$ is an unexplored and important channel to study due to its parity violation, allowing for the construction of an asymmetry, thus allowing for measurement of polarization observables.
- Polarization observables allow for the disentanglement of N^* and Δ^* resonances.
- Determination of observables leads an understanding of the intermediate steps involved in the reaction of interest.
- Double polarization observables C_x and C_z have never measured for the $K^0\Sigma^+$ channel.

Summary

- The photoproduction of $K^0\Sigma^+$ is an unexplored and important channel to study due to its parity violation, allowing for the construction of an asymmetry, thus allowing for measurement of polarization observables.
- Polarization observables allow for the disentanglement of N^* and Δ^* resonances.
- Determination of observables leads an understanding of the intermediate steps involved in the reaction of interest.
- Double polarization observables C_x and C_z have never measured for the $K^0\Sigma^+$ channel.
- Current issue lies with the ML fit error bars; C_x/C_z observables appear to be consistent with zero. We seek to address what becomes of this "missing" polarization.

Thank you so much for your time!